Journal of Environmental Sciences 26 (2014) 1188–1194

Available online at www.sciencedirect.com

Journal of Environmental Sciences

www.jesc.ac.cn

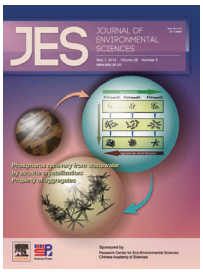

Efficient dechlorination of chlorinated solvent pollutants under UV irradiation by using the synthesized TiO_2 nano-sheets in aqueous phase

Landry Biyoghe Bi Ndong[1], Murielle Primaelle Ibondou[1], Zhouwei Miao[1], Xiaogang Gu[1], Shuguang Lu[1,*], Zhaofu Qiu[1], Qian Sui[1], Serge Maurice Mbadinga[2]

1. State Environmental Protection Key Laboratory of Environmental Risk Assessment and Control on Chemical Process, East China University of Science and Technology, Shanghai 200237, China. E-mail: biyoghendong@gmail.com

2. State Key Laboratory of Bioreactor Engineering and Institute of Applied Chemistry, East China University of Science and Technology, Shanghai 200237, China

ARTICLE INFO

Article history:
Received 03 July 2013
revised 29 October 2013
accepted 08 November 2013

Keywords:
photo-degradation
TiO_2
chlorinated solvent pollutants
nitrobenzene
UV illumination
groundwater remediation

DOI: 10.1016/S1001-0742(13)60541-0

ABSTRACT

Titanium dioxide (TiO_2), which is the widely used photo-catalyst, has been synthesized by simple hydrothermal solution containing tetrabutyl titanate and hydrofluoric acid. The synthesized product has been applied to photo-degradation in aqueous phase of chlorinated solvents, namely tetrachloroethene (PCE), trichloroethene (TCE) and 1,1,1-trichloroethane (TCA). The photo-degradation results revealed that the degradation of these harmful chemicals was better in UV/synthesized TiO_2 system compared to UV/commercial P25 system and UV only system. The photo-catalytic efficiency of the synthesized TiO_2 was 1.4, 1.8 and 3.0 folds higher compared to the commercial P25 for TCA, TCE and PCE degradation, respectively. Moreover, using nitrobenzene (NB) as a probe of hydroxyl radical (·OH), the degradation rate was better over UV/synthesized TiO_2, suggesting the high concentration of ·OH generated in UV/synthesized TiO_2 system. In addition, ·OH concentration was confirmed by the strong peak displayed in EPR analysis over UV/synthesized TiO_2 system. The characterization result using XRD and TEM showed that the synthesized TiO_2 was in anatase form and consisted of well-defined sheet-shaped structures having a rectangular outline with a thickness of 4 nm, side length of 50 nm and width of 33 nm and a surface 90.3 m^2/g. XPS analysis revealed that ≡Ti-F bond was formed on the surface of the synthesized TiO_2. The above results on both photo-catalytic activity and the surface analysis demonstrated the good applicability of the synthesized TiO_2 nano-sheets for the remediation of chlorinated solvent contaminated groundwater.

Introduction

Advanced physico-chemical processes using semiconductor photo-catalysis have been applied as a promising technique for decontamination, purification and/or deodorization of polluted water (Griboval et al., 1999; Stock et al., 2000; Rajeshwar et al., 2008; El Saliby et al., 2012; Jung et al., 2013; Naeem and Ouyang, 2013). Among worldwide used photo-catalysts, titanium dioxide (TiO_2) is considered to be the most suitable catalyst due to its non-toxicity, biological and chemical inertness, cheapness, strong oxidizing power and the long-term stability against corrosion.

As in heterogeneous photo-catalysis, oxidation reactions usually take place on the surface of TiO_2, the morphology of the catalyst, which determines the surface area and the structural properties, plays a key role in catalytic activity (Fox and Dulay, 1993; Hoffmann et al., 1995; Linsebigler et al., 1995; Du et al., 2003; Dozzi et al., 2011). As the outer surface of an oxide is covered by hydroxyl groups,

* Corresponding author. E-mail: lvshuguang@ecust.edu.cn

the nature of these surface hydroxyl groups is of great importance in governing the surface reaction. It has also been reported that, post-treated TiO_2 with Brønsted acids such as hydrofluoric acid leads to much higher catalytic activity properties as it determines the surface charge and influences the interaction between polar organic molecules and oxide surfaces (Yu et al., 2009; Wang et al., 2011; Zhang et al., 2011; Lü et al., 2012; Dozzi et al., 2013).

Han et al. (2009) have synthesized titania nano-sheets with a high percentage of exposed (001) facets which have shown good photo-catalytic properties. Shortly after, Xiang et al. (2010) have investigated the influences of hydrofluoric acid content on the microstructures and the photo-catalytic activity of TiO_2 nano-sheets. These materials have shown a very good photo-catalytic activity for the degradation of organic dyes. However, these products have not been applied to a wide range of persistent organic pollutants such as tetrachloroethene (PCE), trichloroethene (TCE) and 1,1,1-trichloroethane (TCA), typically chlorinated solvents which have been commonly used in dry cleaning and degreasing industries as solvents and have constituted a major public health and environmental concerns (Rivett et al., 1990; Doherty, 2000; Tabrez and Ahmad, 2012). Due to their low aqueous solubility, high density and mobility, they are mostly distributed in contaminated soil and groundwater. Moreover, they are known to be resistant to environmental (chemical, physical and biological) degradation, hence being classified as persistent organic pollutants (Wilson et al., 2007; Lu et al., 2011; Chambon et al., 2013). Thus, their release into water without appropriated treatment is very harmful for the ecosystem.

Herein, we investigate the applicability of synthesized TiO_2 nano-sheets on the removal of PCE, TCE and 1,1,1-TCA in the aqueous phase under UV irradiation. TiO_2 nano-sheets have been synthesized by a simple hydrothermal method using tetrabutyl titanate as the precursor and hydrofluoric acid as a reducing and morphology controlling agent. In the present report, the synthesized TiO_2 nano-sheets have been used in the advanced oxidation process. Nitrobenzene was used as a probe to detect the presence of ·OH radical generated over the all systems. Electron paramagnetic resonance (EPR) analysis was conducted over UV/synthesized TiO_2 to confirm the presence ·OH radical. Brunauer-Emmett-Telle (BET) and X-ray photoelectron spectroscopy (XPS) analysis revealed that the synthesized product exhibited high surface area, larger pore size and high hydroxyl radical potential that can provide their application on a wide scale.

1 Materials and methods

1.1 Chemicals

Tetrabutyl-titanate ($Ti(OBu)_4$, 98.0%), hydrofluoric acid (HF, 45.0%), TiO_2-P25 (Degussa), hexane (97.0%), ethanol (95.0%), tetrachloroethene (PCE, 99.0%), trichloroethene (TCE, 99.0%), 1,1,1-trichloroethane (TCA, 99.0%), nitrobenzene (NB) and 5,5-Dimethyl-1-pyrroline N-oxide (DMPO) was purchased from Sigma (Shanghai, China) were purchased from Shanghai Jingchun Reagent Co. Ltd. (China). All chemicals were of analytical grade and used without further purification. Ultrapure water from a Milli-Q water process (Classic DI, ELGA, Marlow, UK) was used in all experiments.

1.2 Catalysts preparation

TiO_2 anatase nano-sheets were synthesized by modifying the hydrothermal method published by Han et al. (2009). In a typical process, 30 mL $Ti(OBu)_4$ and 2 mL HF were mixed in a dried Teflon autoclave with a capacity of 50 mL, and then kept at 180°C for 24 hr. After cooling to room temperature, the grey precipitate was separated by high-speed centrifugation at 3000 r/min for 15 min, washed with ethanol and ultrapure water for several times to remove impurities, and then dried in vacuum at 70°C for 24 hr.

1.3 Characterization

The ·OH radical generated over UV/synthesized TiO_2 was identified by EPR (EMX-8/2.7C, Bruker, Germany) using DMPO as a spin trap. The instrumental settings were as follows: field sweep, 100 G; microwave frequency, 9.866 GHz; microwave power, 2.016 mW; modulation amplitude, 1 G; conversion time, 40.96 msec; time constant, 163.84 msec; receiver gain, 3.17 × 104; and number of scans, 1. The phase structure and phase purity of the synthesized products were examined by X-ray diffraction (XRD), using a Rigaku D/max 2550VB/PC diffractometer with Cu$K\alpha$ (λ = 0.154 nm) radiation as the incident beam. The surface chemical bonding was characterized by XPS measurement using a Thermo Fisher ESCALAB 250xi with a cylindrical mirror analyzer and an Al $K\alpha$ radiation at acceleration voltage of 15 kV to examine the atomic composition and oxidation state of each atom on the surface of synthesized products. The specific surface area and pore size of the materials were obtained by the BET method at liquid nitrogen temperature with a Quantasorb Jr. instrument (Quantachrome Co. UK). Transmission electron microscopy (TEM) was performed on JEM-1400 electron microscope operated at an accelerating voltage at 80 kV.

1.4 Photo-degradation test

The photo-catalytic test was conducted in a 1.0 L cylindrical glass reactor (containing 3 g of photo-catalysts powder and 20 mg/L of pollutant in aqueous solution), with a magnetic stirrer located at the base of the reactor to maintain the solution homogeneity. Two 10 W low-pressure mercury vapor lamp (Guangdong, China) at 254

nm wavelength was used, hereafter, referred to as UV. The aqueous solution was filled into the reactor and the temperature was kept constant at 20°C during all experiments with a cooling water jacket using a thermostat circulating water bath (SCIENTZ SDC-6, Zhejiang, China). Aqueous samples were taken at desired time intervals and analyzed immediately. Before illumination, the suspension was stirred for 15 min in the dark to reach the adsorption-desorption equilibrium between the pollutants and the photo-catalyst.

1.5 Analytical methods

Samples were analyzed following extraction with of hexane (1 mL:1 mL). The samples were mixed with hexane using a vortex stirrer for 3 min, and then allowed to separate by standing for 5 min. The organic phase was then transferred to a 2-mL gas chromatograph (GC) vial with a plastic dropper and quantified by a gas chromatograph (Agilent 7890A, Palo Alto, CA) equipped with an electron capture detector (ECD), an autosampler (Agilent 7693) and a DB-VRX column (60-m length, 320-μm inner diameter, 1.4-μm thickness). The temperatures of the injector and detector were 240°C and 260°C, respectively, and the oven temperature was isothermal at 75°C. The amount of sample injected was 1 μL with a split ratio of 20:1. The concentration of NB was analyzed using the same gas chromatograph (Agilent 7890A, Palo Alto, CA) equipped with an flame ionization detector (FID), an auto-sampler (Agilent 7693), and an HP-5 column (30-m length, 320-μm i.d., 0.25-μm thickness). The temperatures of the injector and detector were 200°C and 250°C respectively, and the oven temperature was constant at 170°C. The amount of sample injected was 1.0 μL with a split ratio of 1:1. The chloride anion was analyzed by ion chromatography (Dionex ICS-I000, Sunnyvale, CA).

2 Results and discussion

2.1 Photo-catalytic activity test

The photo-catalytic test of the synthesized TiO_2 nano-sheets was carried out by degrading 1,1,1-TCA, TCE and PCE. As shown in **Fig. 1**, PCE and TCE can be effectively removed under UV irradiation, however, UV light cannot degrade TCA that is conformed to the reported studies on the photolysis of these organics compounds (Rashid and Sato, 2011; Gu et al., 2013). Moreover, using the synthesized TiO_2 nano-sheets, photo-degradation of the studied chlorinated solvent pollutants was remarkably enhanced. The photo-degradation of TCE and TCA was also enhanced using the commercial P25. The complete photo-degradation of TCA, TCE and PCE occurred within 70, 40 and 10 min over the synthesized TiO_2 nano-sheets. The degradation of chlorinated solvent pollutants followed the first-order kinetic and the rate constants were calculated and showed in **Table 1**. The degradation rate constant of TCA (0.03492 min^{-1}) over the synthesized TiO_2 nano-sheets was the lowest compared to TCE (0.08275 min^{-1}) and PCE (0.3128 min^{-1}). Following the above observations in the present study, the photo-degradation of chlorinated solvents in aqueous phase is in the following trend: TCA < TCE < PCE, which may be due to the specific electrostatic interactions in each chemical.

Dechlorination rate of TCE, i.e. moles of Cl^- released divided by moles of Cl^- in parent TCE, over the synthesized TiO_2 nano-sheets, the commercial P25 and UV photolysis are shown in **Fig. 2**. Compared to the degradation of TCE in **Fig. 1**, the results revealed that the dechlorination rate increased along with the decrease in TCE concentration. Assuming complete dechlorination of 1 mol of TCE produces 3 mol of Cl^-, it was clear that the decomposed TCE was completely dechlorinated within 40 and 60 min over the synthesized TiO_2 nano-sheets and the commercial P25 as the dechlorination rate was completely consistent with theoretical dechlorination rate calculated according to TCE degradation rate (**Fig. 2**). Moreover, no peak was observed as byproduct according to the GC/MS analysis (date not shown here), further suggesting that chlorinated pollutants were completely dechlorinated when UV was coupled with TiO_2 for the removal of TCA, TCE and PCE in aqueous phase.

The high photo-catalytic activity of the synthesized

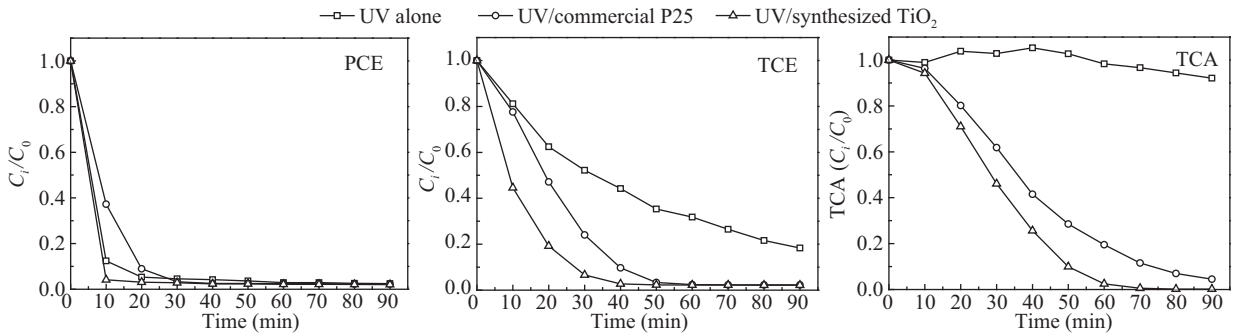

Fig. 1 Photo-degradation performances of PCE, TCE and TCA.

Table 1 Parameters of PCE, TCE and TCA degradation in UV and UV/TiO_2 systems

Operational conditions	Quantity (g)	Degradation rate (%)	Degradation rate constant k (min^{-1})	Correlation coefficient R^2
PCE	–	–	–	–
UV alone	–	100	0.19920	0.9888
Commercial P25	3	100	0.10530	0.9952
Synthesized TiO_2	3	100	0.31280	0.9930
TCE	–	–	–	
UV alone	–	81.64	0.01964	0.9946
Commercial P25	3	100	0.04670	0.9737
Synthesized TiO_2	3	100	0.08275	0.9978
TCA	–	–	–	–
UV alone	–	0.700	–	–
Commercial P25	3	95.48	0.02592	0.9538
Synthesized TiO_2	3	100	0.03492	0.9295

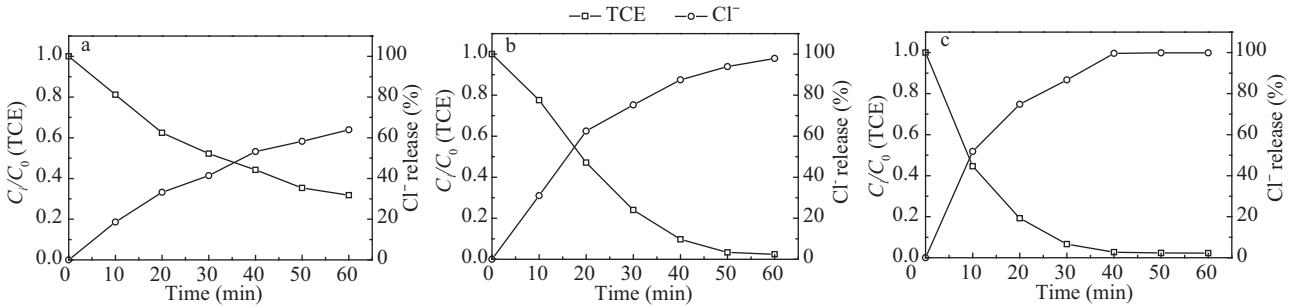

Fig. 2 Comparisons of degradation and dechlorination rate of TCE over (a) UV only, (b) UV/commercial P25 and (c) UV/synthesized TiO_2.

TiO_2 nano-sheets compared to the commercial P25 may be due to the direct photolysis and the direct oxidation by generated oxygen species from water photolysis, as well as the surface ≡Ti–F group on the nano-sheets hand. The efficient photolysis might be the effect of higher photon energy generated by UV light which first breaks chemical bonds, leading to different electronically excited states and vulnerable to attack by oxidation of oxidative species. It is also well known that the surface ≡Ti–F group can reduce the recombination rate of photo-generated electrons and holes, because it can act as an electron-trapping site to trap the photo-generated electrons by tightly holding trapped electrons due to the strong electronegativity of the fluorine and then transferring them to O_2 adsorbed on the surface of TiO_2 (Xiang et al., 2010).

Nitrobenzene (NB) was chosen as a probe to check the presence of ·OH, which is known to be responsible for NB degradation (Legube et al., 1999; Shen et al., 2009; Whang et al., 2012). The photo-degradation test of 0.25 mmol/L for NB aqueous solution was conducted at the same conditions as described for TCE degradation. The photo-degradation curves of NB are shown in **Fig. 3**. Primarily, no degradation of NB was observed over NB/UV alone, NB/commercial P25 and NB/synthesized TiO_2. However, the degradation of NB was observed when the solution was illuminated by UV coupled with the catalysts. The degradation of NB was better (65%) over NB/UV/synthesized

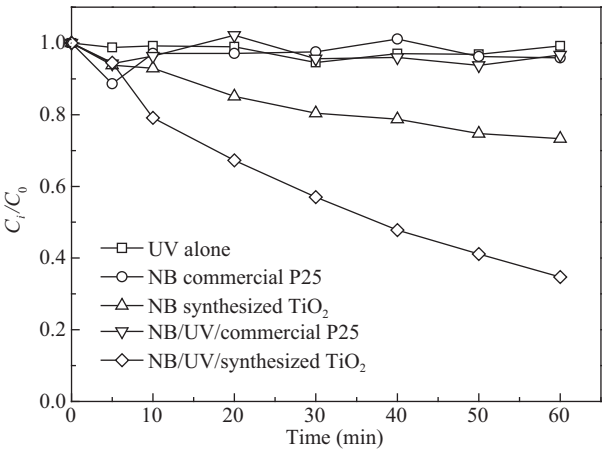

Fig. 3 Photo-degradation of NB in various systems.

TiO_2 after 60 min, suggesting that the intensity of ·OH generated under UV/synthesized TiO_2 was better than that generated under UV alone and UV/commercial P25. Furthermore, according to the NB degradation results over NB/commercial P25 and NB/synthesized TiO_2, it can be concluded that commercial P25 and synthesized TiO_2 are activated only under UV irradiation. EPR analysis was conducted to further confirm the presence of ·OH in the UV/synthesized TiO_2 system using DMPO to trap ·OH radicals. As shown in **Fig. 4**, the observed fourth peaks confirmed the presence of ·OH in the degradation process

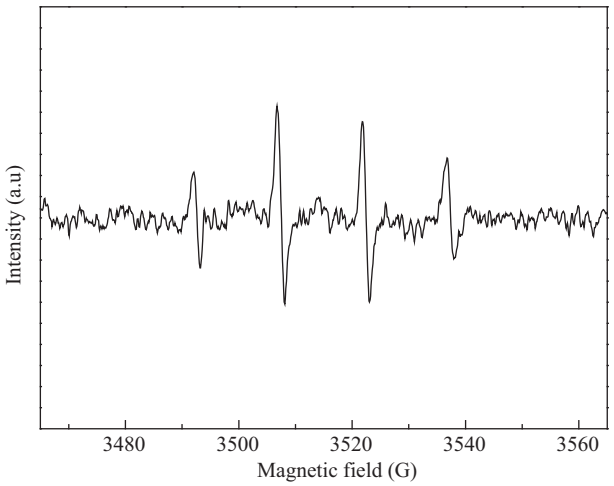

Fig. 4 EPR spectra of ·OH radical trapped by DMPO over UV/synthesized TiO_2.

(Zhai et al., 2011).

2.2 TEM images and X-ray diffraction

The morphology of a photo-catalyst can influence its chemical properties as well. From transmission electron microscopy image shown in **Fig. 5a**, the synthesized TiO_2 consisted of well-defined sheet-shaped structures having a rectangular outline with approximately a thickness of 4 nm, side length of 50 nm and width of 33 nm. **Figure 5b** is the XRD patterns of the synthesized TiO_2. The synthesized TiO_2 exhibited strong diffraction peak that is proved in their high crystallinity (Wang et al., 2012). The diffraction peak at 2θ of 25.3°, 37.8°, 48.1°, 55.1°, 62.7°, 70.3° and 75.1° can be indexed as pure TiO_2 anatase phase (JCPDS No.21-1272) that is confirmed in the work by Han et al. (2009) and Xiang et al. (2010).

BET analysis indicated that the synthesized TiO_2 nano-sheets have a relatively large surface area of 90.3 m^3/g and pore volume of 0.3 cm^3/g. These observations are conformed to the studies by Xiang et al. (2010) for the shape and morphology controlling agent of HF. Recently, similar effect of HF on the TiO_2 growth has been observed (Jiao et al., 2012). In this study, a relatively low volume of HF (2 mL) has been used for the synthesis of TiO_2 nano-sheets.

Besides the role played by F^- anions, the above morphology can also explain the relatively high photo-catalytic activity of the synthesized TiO_2 nano-sheets. As in heterogeneous photo-catalysis, oxidation reactions usually take place on the surface of TiO_2; the chlorinated solvent pollutants are adsorbed on the surface of nano-sheets and later, are easily degraded due to the uniform illumination on the surface of TiO_2 nano-sheets.

2.3 XPS characterization

In order to thoroughly investigate the photo-catalytic activity performance of the synthesized products, we further examined the change in surface chemical bonding of the TiO_2 nano-sheets by XPS. The XPS spectra of the synthesized TiO_2 nano-sheets are displayed in **Fig. 6**. As shown in **Fig. 6a**, the respective photo-electron peaks binding energies of F, Ti, O and C elements were found to be 682.6 eV (F1s), 458.6 eV (Ti2p), 531.7 eV (O1s), 284.8 eV (C1s). **Figure 6b** and **c** is the scan spectra of Ti2p and O1s respectively.

The binding energies of $Ti2p_{3/2}$ and $Ti2p_{1/2}$ are clearly identified at 458.6 and 464.3 eV respectively, which are attributed to the Ti^{4+} oxidation states of TiO_2. This is in agreement with the literature for the anatase phase (Xiang et al., 2010). The detected fluorine species identified in **Fig. 4a** can be attributed to the ≡Ti-F surface bonds formed by ligand exchange reaction between F^- and the surface hydroxyl group on the surface of TiO_2 (Xiang et al., 2010; Wang et al., 2011). Carbon peak is attributed to the residual carbon from the sample and adventitious hydrocarbon from the XPS instrument itself, while, the peak of O1s is attributed to O_{II} to surface adsorbed oxygen (O^{2-} or O^-), ^-OH groups and oxygen vacancies (Kim et al., 2010;

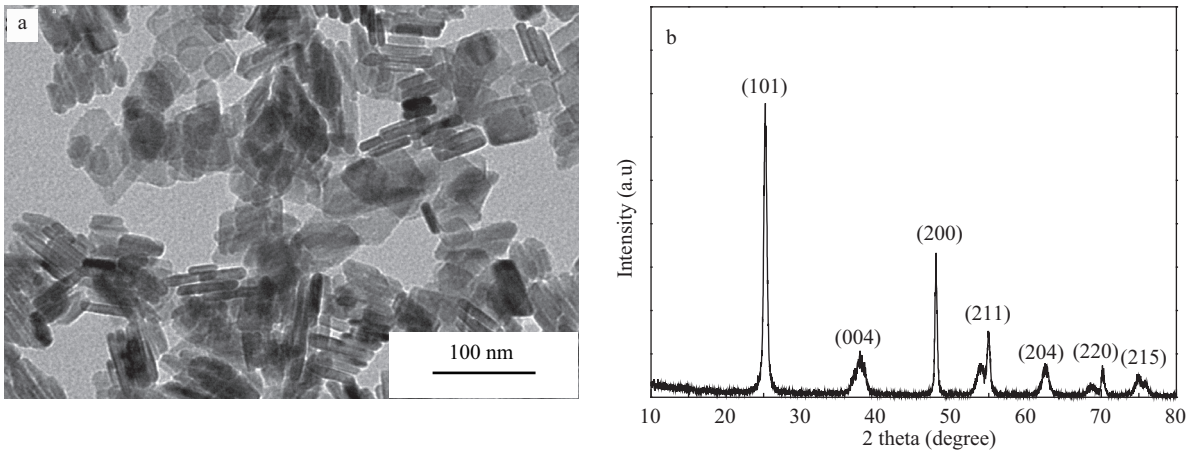

Fig. 5 (a) TEM image and (b) XRD patterns of the synthesized TiO_2 anatase nano-sheets.

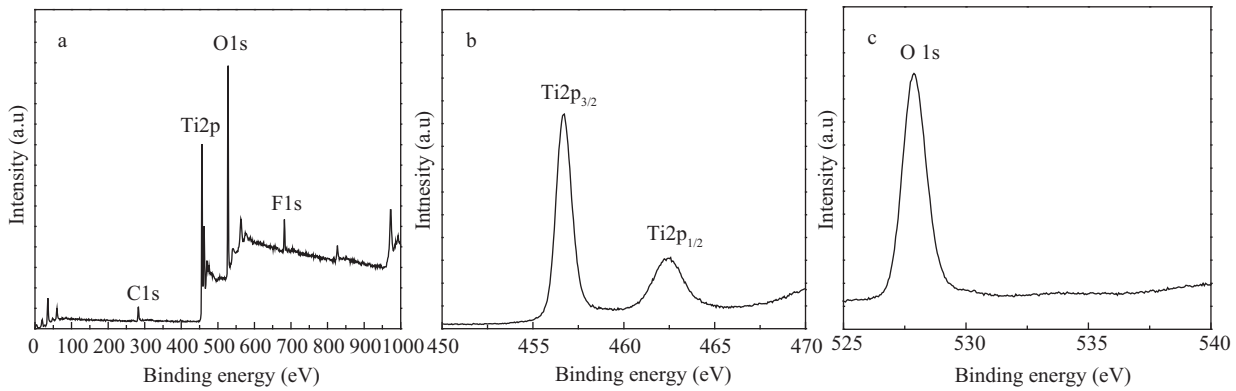

Fig. 6 (a) XPS survey spectra, (b) XPS scan spectra of Ti2P and (c) XPS scan spectra of O1s of the synthesized TiO_2 anatase nano-sheets.

Monteagudo et al., 2011). The above information can explain the good photo-catalytic activity of the synthesized TiO_2 nano-sheets by the degradation of chlorinated solvent pollutants and nitrobenzene as reported by Rashid and Sato (2011). Moreover it was found that the substitution of the surface hydroxyl groups by F^- anions on the TiO_2 surfaces enhanced the formation of ·OH free radicals, which is conformed to the EPR analysis. The strong adsorption of F^- anions on the surface of TiO_2 and the high potential of the couple $F^•/F^-$ (3.6 V) can cause fluorine ions to be stable against oxidation by TiO_2 valence holes.

3 Conclusions

In the present study, TiO_2 anatase nano-sheets have been synthesized by a simple hydrothermal method and their photo-catalytic activities have been tested by degrading three chlorinated solvent pollutants, namely TCA, TCE and PCE in aqueous solution. The photo-degradation rate of the tested chlorinated solvent pollutants was the highest when UV light was coupled with the synthesized TiO_2 nano-sheets. The degradation rate which was in the following trend of TCA < TCE < PCE suggested that TCA was the most recalcitrant chlorinated solvent pollutant. Moreover, the degradation result of NB, which was better over UV/synthesized TiO_2, demonstrated the hydroxyl radicals were only generated when UV was coupled with catalyst. The strong peaks displayed by EPR analysis conducted on UV/synthesized TiO_2 further confirmed the generation of ·OH radicals in UV/synthesized TiO_2 system. The characterization analyses by XRD, TEM and BET have shown the good crystallite and the anatase phase of the synthesized TiO_2 nano-sheets which exhibited a large surface area. XPS analysis has revealed that the formation of the ≡Ti-F surface bonds is highly responsible for the excellent photo-catalytic efficiency of the synthesized product as it promotes the formation of hydroxyl radicals. The experimental results proposed the simple and economical method to synthesis new photo-catalyst for wide application in groundwater remediation.

Acknowledgments

This work was supported by the National Environmental Protection Public Welfare Science and Technology Research Program of China (No. 201109013), the National Natural Science Foundation of China (No. 41373094, 51208199), the Shanghai Natural Science Funds (No. 12ZR1408000), the China Postdoctoral Science Foundation (No. 2013T60429) and the China Scholarship Council for PhD program at East China University of Science Technology.

REFERENCES

Chambon, J.C., Bjerg, P.L., Scheutz, C., Bælum, J., Jakobsen, R., Binning, P.J., 2013. Review of reactive kinetic models describing reductive dechlorination of chlorinated ethenes in soil and groundwater. Biotechnol. Bioeng. 110(1), 1–23.

Doherty, R.E., 2000. A history of the production and use of carbon tetrachloride, tetrachloroethylene, trichloroethylene and 1,1,1-trichloroethane in the United States: Part 2-Trichloroethylene and 1,1,1-Trichloroethane. Env. Forensics 1(2), 83–93.

Dozzi, M., Selli, E., 2013. Specific facets-dominated anatase TiO_2: Fluorine-mediated synthesis and photoactivity. Catalysts 3(2), 455–485.

Dozzi, M.V., Livraghi, S., Giamello, E., Selli, E., 2011. Photocatalytic activity of S- and F-doped TiO_2 in formic acid mineralization. Photochem. Photobiol. Sci. 10(3), 343–349.

Du, Y., Rabani, J., 2003. The Measure of TiO_2 photocatalytic efficiency and the comparison of different photocatalytic titania. J. Phys. Chem. B 107(43), 11970–11978.

El Saliby, I., Shahid, M., McDonagh, A., Shon, H.K., Kim, J.H., 2012. Photodesorption of organic matter from titanium dioxide particles in aqueous media. J. Industr. Eng. Chem. 18(5), 1774–1780.

Fox, M.A., Dulay, M.T., 1993. Heterogeneous photocatalysis. Chem. Rev. 93(1), 341–357.

Griboval, A., Blanchard, P., Gengembre, L., Payen, E., Fournier, M., Dubois, J.L. et al., 1999. Hydrotreatment catalysts prepared with heteropolycompound: Characterisation of the oxidic precursors. J. Catal. 188(1), 102–110.

Gu, X., Lu, S., Qiu, Z., Sui, Q., Banks, C.J., Imai, T. et al., 2013. Photodegradation performance of 1, 1, 1-trichloroethane in aqueous solution: In the presence and absence of persulfate. Chem. Eng. J. 215–216, 29–35.

Han, X.G., Kuang, Q., Jin, M.S., Xie, Z.X., Zheng, L.S., 2009. Synthesis of titania nanosheets with a high percentage of exposed (001) facets and related photocatalytic properties. J. Am. Chem. Soc. 131(9), 3152–3153.

Hoffmann, M.R., Martin, S.T., Choi, W., Bahnemann, D.W., 1995. Environmental applications of semiconductor photocatalysis. Chem. Rev. 95(1), 69–96.

Jiao, W., Wang, L., Liu, G., Lu, G.Q., Cheng, H.M., 2012. Hollow anatase TiO_2 single crystals and mesocrystals with dominant {101} facets for improved photocatalysis activity and tuned reaction preference. ACS. Catal. 2(9), 1854–1859.

Jung, H.J., Hong, J.S., Suh, J.K., 2013. A comparison of fenton oxidation and photocatalyst reaction efficiency for humic acid degradation. J. Indust. Eng. Chem. 19(4), 1325–1330.

Kim, S.U., Liu, Y.P., Nash, K.M., Zweier, J.L., Rockenbauer, A., Villamena, F.A., 2010. Fast reactivity of a cyclic nitrone-calix[4]pyrrole conjugate with superoxide radical anion: theoretical and experimental studies. J. Am. Chem. Soc. 132(48), 17157–17173.

Legube, B., Karpel Vel Leitner, N., 1999. Catalytic ozonation: a promising advanced oxidation technology for water treatment. Catal. Today 53(1), 61–72.

Linsebigler, A.L., Lu, G., Yates, J.T., 1995. Photocatalysis on TiO_2 surfaces: principles, mechanisms, and selected results. Chem. Rev. 95(3), 735–758.

Lu, C., Bjerg, P.L., Zhang, F., Broholm, M.M., 2011. Sorption of chlorinated solvents and degradation products on natural clayey tills. Chemosphere 83(11), 1467–1474.

Lü K., Cheng, B., Yu, J.G., Liu, G., 2012. Fluorine ions-mediated morphology control of anatase TiO2 with enhanced photocatalytic activity. Phys. Chem. Chem. Phys. 14(16), 5349-5362.

Monteagudo, J.M., Durán, A., Aguirre, M., San Martín, I., 2011. Optimization of the mineralization of a mixture of phenolic pollutants under a ferrioxalate-induced solar photo-Fenton process. J. Hazard. Mater. 185(1), 131–139.

Naeem, K., Ouyang, F., 2013. Influence of supports on photocatalytic degradation of phenol and 4-chlorophenol in aqueous suspensions of titanium dioxide. J. Environ. Sci. 25(2), 399–404.

Rajeshwar, K., Osugi, M.E., Chanmanee, W., Chenthamarakshan, C.R., Zanoni, M.V.B., Kajitvichyanukul, P. et al., 2008. Heterogeneous photocatalytic treatment of organic dyes in air and aqueous media. J. Photochem. Photobiol. C 9(4), 171–192.

Rashid, M.M., Sato, C., 2011. Photolysis, Sonolysis, and Photosonolysis of Trichloroethane (TCA), Trichloroethylene (TCE), and Tetrachloroethylene (PCE) without catalyst. Water. Air. Soil. Pollut. 216(1-4), 429–440.

Rivett, M.O., Lerner, D.N., Lloyd, J.W., 1990. Chlorinated solvents in UK aquifers. Water Environ. J. 4(3), 242–250.

Shen, X.Z., Liu, Z.C., Xie, S.M., Guo, J., 2009. Degradation of nitrobenzene using titania photocatalyst co-doped with nitrogen and cerium under visible light illumination. J. Hazard. Mater. 162(2-3), 1193–1198.

Stock, N.L., Peller, J., Vinodgopal, K., Kamat, P.V., 2000. Combinative sonolysis and photocatalysis for textile dye degradation. Environ. Sci. Technol. 34(9), 1747–1750.

Tabrez, S., Ahmad, M., 2012. Genotoxicity of trichloroethylene in the natural milieu. Int. J. Hyg. Environ. Health. 215(3), 333–338.

Wang, G., Xu, L., Zhang, J., Yin, T., Han, D., 2012. Enhanced photocatalytic activity of TiO_2 powders (P25) via calcination treatment. Int. J. Photoenergy, Article ID 265760, 2012, DOI:10.1155/2012/265760.

Wang, Y., Zhang, H.M., Han, Y.H., Liu, P., Yao, X.D., Zhao, H.J., 2011. A selective etching phenomenon on {001} faceted anatase titanium dioxide single crystal surfaces by hydrofluoric acid. Chem. Commun. 47(10), 2829–2831.

Whang, T.J., Hsieh, M.T., Shi, T.E., Kuei, C.H., 2012. UV-Irradiated photocatalytic degradation of nitrobenzene by titania binding on quartz tube. Int. J. Photoenergy. Article ID 681941, 2012. DOI: 10.1155/2012/681941.

Wilson, K., Sewell, G., Kean, J.A., Vangelas, K., 2007. Enhanced attenuation: Its place in the remediation of chlorinated solvents. Remed. J. 17(2), 39–49.

Xiang, Q., Lv K., Yu, J., 2010. Pivotal role of fluorine in enhanced photocatalytic activity of anatase TiO_2 nanosheets with dominant (001) facets for the photocatalytic degradation of acetone in air. Appl. Catal. B 96(3-4), 557–564.

Yu, J., Wang, W., Cheng, B., Su, B.L., 2009. Enhancement of photocatalytic activity of mesporous TiO_2 powders by hydrothermal surface fluorination treatment. J. Phys. Chem. C 113(16), 6743–6750.

Zhai, Q., Bo, T., Hu, G., 2011. High photoactive and visible-light responsive graphene/titanate nanotubes photocatalysts: Preparation and characterization. J. Hazard. Mater. 198, 78–86.

Zhang, H., Wang, Y., Liu, P., Han, Y., Yao, X., Zou, J. et al., 2011. Anatase TiO_2 crystal facet growth: mechanistic role of mydrofluoric acid and photoelectrocatalytic activity. ACS Appl. Mater. Inter. 3(7), 2472–2478.